RACSAM (2014) 108:617–631
DOI 10.1007/s13398-013-0130-x

ORIGINAL PAPER

A numerical approach to solve an inverse problem in lubrication theory

Hassán Lombera · J. Ignacio Tello

Received: 24 January 2013 / Accepted: 17 May 2013 / Published online: 15 June 2013

Abstract In this paper we consider a numerical approach to reach the equilibrium position of a journal bearing with radial loading. The system consists of an external cylinder surrounding a rotating shaft. The problem is modelled by the hydrodynamic Reynolds equation with a cavitation model of Elrod–Adams. Both equations are coupled to Newton's second law which describes the position of the shaft. The problem is considered as an inverse problem where the coefficient of the equation is unknown. The numerical approach to solve the inverse problem is based on a trust-region algorithm along with the finite element method. The Heaviside function in the Elrod–Adams equation is approximated by a third order Hermite polynomial. The trust-region algorithm for solving the inverse problem showed another way of solution, different from the ones that exist at this moment.

Keywords Cavitation · Elrod–Adams model · Finite element method · Inverse problem · Journal bearing · Trust-region algorithm

Mathematics Subject Classification (2000) 65M32 · 65M25 · 49J10

1 Introduction

The device consists of an external cylinder which surrounds a rotating shaft in relative motion. Both are closely spaced and the annular gap between them is filled with a lubricant to prevent the contact. Journal bearings are used extensively for load support of rotating machinery like thermal engines, compressors or gear boxes.

H. Lombera (✉)
Center of Computer Science Applied to Industry, Faculty 5,
University of Computer Science, Havana 19370, Cuba
e-mail: hlombera@uci.cu

J. I. Tello
Matemática Aplicada, E.U.I. Informática,
Universidad Politécnica de Madrid, Madrid 28031, Spain
e-mail: jtello@eui.upm.es

In this paper we aim to obtain a numerical approach to predict the equilibrium position of the shaft which balances the hydrodynamic load and a given force vector imposed on the device. We consider a stationary regime of a Newtonian, incompressible, isothermal and isoviscous lubricant. Notice that the device should support the forces applied without contact between both surfaces. Technical problems on those devices entail stopping a productive machine, a disassembly process, and in general a waste of economical resources. This work is a first step to understanding the vast problem of journal bearing with an imposed load. The stability of the steady state is not addressed here. Nevertheless, it is an interesting question that will be considered for future work. Other interesting questions remain open, as the global existence of the time dependent problem or finite time contact. Concerning the direct problem, roughness is also one of the challenges of the field, see for instance [4,5] and references there in.

Mathematical models in Lubrication Theory assume that the unknown pressure p is constant through the thickness of the fluid film, which allows one to approximate the three dimensional Navier–Stokes equations by the bidimensional Reynolds equation (see [2] for details). In lubrication, cavitation is one of the most relevant processes with important economical implications in industry because of its effects. It is defined in Dowson–Taylor [13] as the rupture of the continuous fluid film due to the formation of air bubbles inside, which makes the Reynolds equation no longer valid in the cavitation area. One of the most used models to describe cavitation is the Elrod–Adams model [19].

In [19], the authors introduce the hypothesis that the cavitation region is a fluid–air mixture and an additional unknown θ appears (the saturation of fluid in the mixture). This model, which still relies on the Reynolds equation has been widely used in Tribology [21]. Unlike some other models, such as the variational inequality model, it does allow the starvation phenomena to take place. Its interest also relies on the evidence that it is a mass-preserving model. In [1,17] comparisons for journal bearings are made, between their operating parameters computed by the variational inequality and Elrod–Adams models.

Numerical methods for solving the Elrod–Adams model for cavitation in different devices and conditions were presented in [3,7,17,18], among others. Similarly, numerical experimentations of various schemes based both on stationary upwind methods and pseudo-stationary techniques were conducted in [10].

These methods are mainly based on the characteristics discretization for the nonlinear convection term and a duality method for the multivalued nonlinear saturation-pressure relation, posed by the Heaviside operator. Namely, they use an approach based on the (MC) to discretize a total derivative in the final formulation. This technique was also used in [14–16] among others, and it is the strategy we chose to solve the problem as well. Additionally, they use a Yosida regularization for the Heaviside operator like in [8]. In contrast, we use a regularization of this function by a cubic interpolating Hermite polynomial that allows us to express the solution of the direct problem as a minimum of a convex functional. Section 3.2 is devoted to this new strategy.

On the other hand, most of the papers previously mentioned deal with imposed geometry in the associated Reynolds equation, i.e. the gap function h for the journal bearing is a given datum and the unknown is the pressure p. In real engineering applications the position of the shaft in a journal bearing, that defines the gap function h, is unknown. So, Newton's second law is introduced to obtain that position. The problem consists in finding the pressure of the lubricant, the concentration function ϑ in the cavitation area and the shaft position. The problem is considered as an inverse problem where the coefficient h depends on the unknown p (see [14,16]). In [16] the authors used an implicit Euler method to deal with the dynamical shaft problem coupled with the fluid hydrodynamic problem. At each time step the resulting

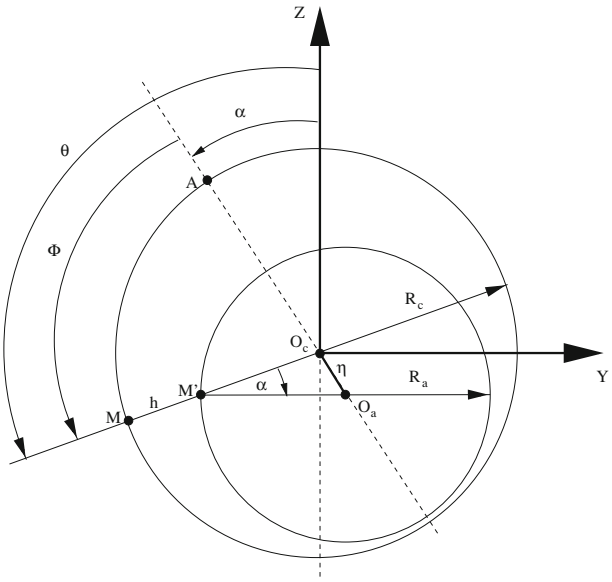

Fig. 1 Cross section of a journal bearing

nonlinear system is solved by the Broyden method combined with the Armijo–Goldstein criterion to choose a proper step length in the descent direction. Note that this is a line-search strategy. In Sect. 4, we propose a different approach to deal with this problem. It is based on first solving the Elrod–Adams equation for a known position by minimizing a convex and lower semi-continuous (l.s.c.) functional and then using an iterative method to reach the equilibrium, namely a trust-region strategy.

In a sense, the line search and trust-region approaches differ in the order in which they choose the direction and distance of the move to the next iterate. Line search starts by fixing the direction and then identifying an appropriate distance (the step length). The trust-region approach chooses a maximum distance, named the trust-region radius $\triangle k$, and then seek a direction and step that attain the best improvement possible subject to this distance constraint. If this step proves to be unsatisfactory, we reduce the distance measure $\triangle k$ and try again. We remark that both approaches are two of the fundamental strategies used in optimization algorithms to generate a sequence of iterates [23].

The outline of the paper is the following. In Sect. 2 we describe the problem of loaded journal bearing systems for stationary regime and pose a suitable variational formulation for the hydrodynamic problem. In Sect. 3, we consider a finite element discretization and solve the direct problem by using an approximation of the Heaviside function. Section 4 is devoted to explaining the resolution of the inverse problem by a trust region algorithm. Numerical test and discussion are provided in Sect. 5.

2 Mathematical model

2.1 Hydrodynamic model

In this section, we depict a 2D formulation of the hydrodynamic behaviour of lubricated journal bearings. Figure 1 shows the cross section of a journal bearing. The inner cylinder,

the shaft of radius R_a, rotates in counterclockwise direction. The film pressure generated by the moving surfaces forces the lubricant through a wedge shaped zone of thickness h, which varies according to the angle α.

We assume a coordinate system in which y represents a circumferential coordinate, z is a coordinate across the fluid film and x depicts the journal bearing axial dimension, orthogonal to the plane zy. The origin of coordinate y is located over the centers line $\overline{O_c O_a}$, to place the minimum gap of the device at an angle $\Phi = \pi$. On the other hand, the reference $z = 0$ is taken on the bearing surface.

To simplify the computations, we introduce the following nondimensional variables

$$\theta = \frac{y}{R_a}, \quad r = \frac{z}{h}, \quad \bar{x} = \frac{x}{L}, \quad \bar{u} = \frac{u}{\omega R_a}, \quad \bar{v} = \frac{v}{\omega C}, \quad \bar{w} = \frac{w}{\omega R_a}, \tag{1}$$

where L represents the shaft length, C the radial clearance, h the fluid film thickness, (u, v, w) the fluid velocity components and ω the angular speed. In addition, other functions and coefficients are defined in relation to the dimensionless properties:

$$\bar{h} = \frac{h}{\omega C}, \quad \lambda = \frac{L}{R_a}, \quad \bar{\mu} = \frac{\mu}{\mu_0}, \quad \bar{p} = \frac{pC^2}{\mu_0 \omega R_a^2}, \tag{2}$$

where μ denotes the viscosity, p is the fluid pressure and λ gives the ratio between the journal radius and length.

The domain is transformed into a nondimensional domain $\Omega = [0, 2\pi] \times [0, 1]$ for the (θ, x) coordinates, where the height is posed as:

$$\bar{h} = 1 + \eta \cos(\theta - \alpha), \tag{3}$$

where η stands for the eccentricity coefficient, defined as $\frac{\overline{O_c O_a}}{C}$.

The governing equations for modelling the dynamic behaviour of a journal bearing system for small fluid film thickness is the generalized Reynolds equation discussed in [20]. The system takes the following form in the geometrical system $(\theta, r, \bar{x})$ for Newtonian fluids with constant density (see [12]).

$$\frac{\partial}{\partial \theta}\left(\bar{h^3}\bar{F}_2 \frac{\partial \bar{p}}{\partial \theta}\right) + \frac{1}{\lambda^2}\frac{\partial}{\partial \bar{x}}\left(\bar{h^3}\bar{F}_2 \frac{\partial \bar{p}}{\partial \bar{x}}\right) = \frac{\partial}{\partial \theta}\left(\bar{h}\left[1 - \frac{\bar{F}_1}{\bar{F}_0}\right]\right), \tag{4}$$

where

$$\bar{F}_2 = \int_0^1 \frac{r}{\bar{\mu}}\left(r - \frac{\bar{F}_1}{\bar{F}_0}\right) \mathrm{d}r, \quad \bar{F}_1 = \int_0^1 \frac{r}{\bar{\mu}} \mathrm{d}r, \quad \bar{F}_0 = \int_0^1 \frac{\mathrm{d}r}{\bar{\mu}} \tag{5}$$

and $\bar{\mu}$ stands for the fluid constant viscosity.

We transform the domain into $\Omega = [0, 2\pi] \times [0, \lambda]$ by introducing the new variable $\tilde{x} = \bar{x}\lambda$. The cavitation phenomena are described by the Elrod–Adams model (see [6] for details). It introduces an additional unknown, the saturation ϑ that represents the lubricant concentration. Namely, it takes the value 1 in the lubricated region Ω^+ and takes any other value in the range [0, 1] within the cavitated region Ω^0, Σ depicts the free boundary between the lubricated region (Ω^+) and the cavitated one (Ω^0); $\vec{n}$ is the normal vector to Σ, $\vec{i}$ is the

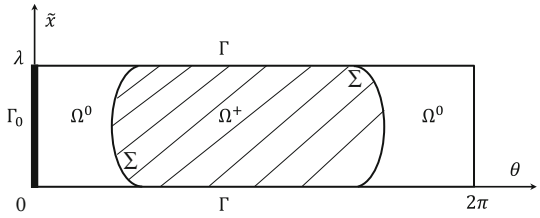

Fig. 2 Hydrodynamic domain configuration

unitary normal vector pointing to θ direction and Γ_0 is the boundary where lubricant is supplied through. See Fig. 2 for details.

So, the hydrodynamic problem with cavitation is posed as follows:
To find (p, ϑ) such that:

$$\frac{\partial}{\partial\theta}\left(\bar{h^3}\bar{F}_2\frac{\partial\bar{p}}{\partial\theta}\right)+\frac{\partial}{\partial\bar{x}}\left(\bar{h^3}\bar{F}_2\frac{\partial\bar{p}}{\partial\bar{x}}\right)=\frac{\partial}{\partial\theta}\left(\bar{h}\left[1-\frac{\bar{F}_1}{\bar{F}_0}\right]\right),\ \bar{p}>0\quad\text{and}\quad\vartheta=1\qquad\text{in}\quad\Omega^+, \tag{6}$$

$$\frac{\partial}{\partial\theta}\left(\vartheta\bar{h}\left[1-\frac{\bar{F}_1}{\bar{F}_0}\right]\right)=0,\quad\bar{p}=0,\quad 0\le\vartheta\le 1\qquad\text{in}\quad\Omega^0, \tag{7}$$

$$\bar{h^3}\bar{F}_2\frac{\partial\bar{p}}{\partial\vec{n}}=(1-\vartheta)\bar{h}\left(1-\frac{\bar{F}_1}{\bar{F}_0}\right)\cos(\vec{n},\vec{i}),\quad\bar{p}=0\qquad\text{on}\quad\Sigma, \tag{8}$$

$$\bar{p}=0\quad\text{on}\quad\Gamma,\quad\vartheta=\vartheta_0\ \text{and}\ p=p_f\quad\text{on}\quad\Gamma_0, \tag{9}$$

where ϑ_0 and p_f stand for the concentration on the groove supply and feeding pressure respectively.

We define the parameter $\Lambda=\frac{1}{\bar{F}_2}\left(1-\frac{\bar{F}_1}{\bar{F}_0}\right)$ and drop the superscripts $\bar{}$ of dimensionless variables to simplify the notation. Then, we introduce the weak formulation of the problem:

Given $\vartheta_0\in L^2(\Gamma_0)$, verifying $0\le\vartheta_0\le 1$, to find $p\in H^1(\Omega)$, 2π-periodic in θ, $p=0$ on Γ and $\vartheta\in L^\infty(\Omega)$ such that:

$$\begin{aligned}\int_\Omega h^3\nabla p\nabla\phi &= \int_\Omega(\vartheta h\Lambda)\frac{\partial\phi}{\partial\theta}+\int_{\Gamma_0}(\vartheta_0 h\Lambda)\phi,\quad\forall\phi\in V,\\ \vartheta\in H(p) &= \begin{cases}1 & :(p>0),\\ [0,1] & :(p=0),\\ 0 & :(p<0),\end{cases}\end{aligned} \tag{10}$$

where the space of test functions is given by:

$$V=\{\phi\in H^1(\Omega)/\phi|_{\Gamma-\Gamma_0}=0\}.$$

2.2 Shaft stationary model

The balance of forces acting on a journal bearing is posed by Newton's second law:

$$\sum_{i=1}^{n}\vec{f}=m\frac{d^2\vec{s}}{dt^2}, \tag{11}$$

where $\vec{f_i}$ (for $i=1\ldots n$) represents the forces applied upon the system.

Thus, at the equilibrium position, i.e. $\frac{d^2\vec{s}}{dt^2} = 0$, the balance of forces is null. So, the load applied to the system "$f = (f_\theta, f_x)$" is equal to the force exerted by the pressure to the shaft given by $(\int_\Omega p(\theta, x)\cos\theta \mathrm{d}\theta\mathrm{d}x, \int_\Omega p(\theta, x)\sin\theta \mathrm{d}\theta\mathrm{d}x)$ i.e.

$$\int_\Omega p(\theta, x)\cos\theta \mathrm{d}\theta\mathrm{d}x = f_\theta, \tag{12}$$

$$\int_\Omega p(\theta, x)\sin\theta \mathrm{d}\theta\mathrm{d}x = f_x, \tag{13}$$

where f_θ and f_x stand for the nondimensional components of the applied external load $\vec{f}$. Integrals stand for the force components generated by the lubricant pressure.

3 Discretization of the hydrodynamic model

By using integration by parts it is possible to rewrite Eq. (10) as follows:

$$\begin{aligned} \int_\Omega h^3 \nabla p \nabla \phi &= -\int_\Omega \frac{\partial}{\partial\theta}(\vartheta h \Lambda)\phi, \quad \forall \phi \in V, \\ \vartheta &= \vartheta_0 \quad \text{in} \quad \Gamma_0. \end{aligned} \tag{14}$$

For the numerical solution of Eq. (14), several techniques have been proposed. Mainly, the existing literature combine the MC with the FEM. To introduce the MC to the problem in the stationary case, we have adopted the technique based on introducing an artificial dependence of time. In this manner, we define:

$$\begin{aligned} \hat{\phi}(\theta, x, t) &= \phi(\theta, x), \\ \hat{p}(\theta, x, t) &= p(\theta, x), \\ \hat{h}(\theta, t) &= h(\theta), \\ \hat{\vartheta}(\theta, t) &= \vartheta(\theta). \end{aligned}$$

Thus, we can write the right-hand side of Eq. (14) in terms of the total derivative, assuming an artificial velocity $v = 1$. So,

$$\frac{D}{Dt} = \frac{\partial}{\partial t} + v\frac{\partial}{\partial\theta} = \frac{\partial}{\partial t} + \frac{\partial}{\partial\theta},$$

then, in the case of a stationary regime we have:

$$\frac{D}{Dt} = \frac{\partial}{\partial\theta}.$$

For simplicity in the notation we drop the superscripts $\hat{}$ of variables from now on. Thus, the problem in Eq. (14) is formulated as the stationary state of the following transient problem:

$$\begin{aligned} \int_\Omega h^3 \nabla p \nabla \phi &= -\int_\Omega \frac{D}{Dt}(\vartheta h \Lambda)\phi, \quad \forall \phi \in V, \\ \vartheta &= \vartheta_0 \quad \text{in} \quad \Gamma_0. \end{aligned} \tag{15}$$

3.1 The method of characteristics

Let $\chi(\theta, t; \tau)$ denote the position at time τ of a particle of fluid moving according to the velocity field v, and placed at the point θ at the reference time t. That is, χ is the solution to the final value problem:

$$\frac{\partial}{\partial \tau}\Big(\chi(\theta, t; \tau)\Big) = v(\chi(\theta, t; \tau)),$$
$$\chi(\theta, t; t) = \theta.$$

So, the approximation of the total derivative is accomplished by using an upwind schema which follows the trajectory (or characteristics) of particles being analyzed.

We introduce the following notation:

- $\triangle t$ is the time step.
- $t^n = n\triangle t$.
- $\chi^n(\theta) = \chi(\theta, t^{n+1}; t^n)$ denotes the position at time t^n of a particle placed at the point θ at time t^{n+1}, when it moves according to the artificial velocity field v.
- $g^{n+1}(\theta) = g(\theta, (n+1)\triangle t)$.

With the above notation we consider:

$$\frac{Dg}{Dt}(\theta, t^{n+1}) \approx \frac{g^{n+1}(\theta) - g^n(\chi^n(\theta))}{\triangle t}. \tag{16}$$

As in fact the time dependence is fictitious, functions $g^{n+1}(\theta)$ and $g^n(\theta)$ are the same, and thereby we can recast Eq. (16) as:

$$\frac{Dg}{Dt}(\theta) \approx \frac{g(\theta) - g(\chi^k(\theta))}{k}, \tag{17}$$

where k plays the role of the artificial time step and $\chi^k(\theta)$ denotes the position at time $t - k$ of a particle placed at the point θ at time t.

Then, substituting Eq. (17) into Eq. (15) yields k-dependent problem sets, that approximate the original problem in Eq. (15) as:

$$\int_\Omega h^3 \nabla p \nabla \phi + \frac{1}{k}\int_\Omega \vartheta h \Lambda \phi = \frac{1}{k}\int_\Omega \left(\vartheta h \Lambda\right) \circ \chi^k \phi, \quad \forall \phi \in V, \quad \vartheta \in H(p). \tag{18}$$

At this point we proposed a fixed-point algorithm to define p^{n+1} as the solution of the following problem:

$$\int_\Omega h^3 \nabla p^{n+1} \nabla \phi + \frac{1}{k}\int_\Omega \vartheta^{n+1} h \Lambda \phi = \frac{1}{k}\int_\Omega \left(\vartheta^n h \Lambda\right) \circ \chi^k \phi, \quad \forall \phi \in V, \ \vartheta^{n+1} \in H(p^{n+1}), \tag{19}$$

which in fact is similar to the strategy of making time tends to infinity until reaching the stationary state.

3.2 The regularization approach for the Heaviside function

The problem under study is nonlinear at each time step, because the Heaviside function $H(p)$. A particular regularization technique has been widely used for dealing with the Heaviside

function discontinuity, namely in [10,16] among others. They adopted a duality type method consisting in applying an algorithm proposed by Bermúdez and Moreno [8] with a Yosida regularization for the Heaviside operator.

We propose a regularization approach by a cubic interpolating Hermite polynomial for the Heaviside function, which is derived following a divided difference schema [24]. With that selection we may express the solution as a minimum of a convex functional at each time iteration. On the other hand, a Yosida regularization approach needs a different iterative procedure to deal with since the convexity of the functional could not be guaranteed in the same way. In this manner, we define the approximation function H_ϵ for the Heaviside's as follows:

$$H_\epsilon(s) = \begin{cases} 1 & : (s > \epsilon), \\ \frac{1}{\epsilon^3}(3\epsilon s^2 - 2s^3) & : (0 \le s \le \epsilon), \\ 0 & : (s < 0). \end{cases} \tag{20}$$

So, from now on, $\vartheta_\epsilon = H_\epsilon(p)$.

3.3 The associated functional

In this section we propose a functional whose minimum is the solution to Eq. (19).

Lemma 1 *Let J_ϵ be the following functional:*

$$J_\epsilon(p) = \frac{1}{2}\int_\Omega h^3|\nabla p|^2 + \frac{1}{k}\int_\Omega h\Lambda\Phi_\epsilon(p) - \frac{1}{k}\int_\Omega \left(\vartheta h\Lambda\right)\circ\chi^k p, \tag{21}$$

where function $\Phi_\epsilon(p)$ is defined as:

$$\Phi_\epsilon(s) = \begin{cases} s - \frac{1}{2}\epsilon & : (s > \epsilon), \\ \frac{1}{\epsilon^3}\left(\epsilon s^3 - \frac{1}{2}s^4\right) & : (0 \le s \le \epsilon), \\ 0 & : (s < 0). \end{cases} \tag{22}$$

Then, J_ϵ is convex, l.s.c. and $\lim_{p\to\infty} J_\epsilon(p) = \infty$ for any $\epsilon < 0$.

Proof Notice that Φ_ϵ is C^2, its second derivative is nonnegative and the rest of the terms in J_ϵ are convex and l.s.c. Then, we have that J_ϵ is l.s.c. and convex. A standard argument proves that $\lim_{p\to\infty} J_\epsilon(p) = \infty$. Thanks to Corollary III.20 in [9], p_ϵ (the minimum of J_ϵ) is the unique solution to the penalized problem

$$\begin{aligned} \int_\Omega h^3\nabla p_\epsilon\nabla\phi \;\; + \frac{1}{k}\int_\Omega \vartheta h\Lambda\phi = \frac{1}{k}\int_\Omega (\vartheta_\epsilon h\Lambda)\circ\chi^k\phi, \quad \forall\phi \in V, \\ \vartheta_\epsilon \in H_\epsilon(p_\epsilon). \end{aligned} \tag{23}$$

Since $H_\epsilon \le 1$, we have that p_ϵ is uniformly bounded in $H^1(\Omega)$. So, there exists a subsequence $p_{\epsilon i}$ which converge weakly to p_* which satisfies (18). Since the solution to (18) is unique (see Bayada, Martin, Vázquez [5]) we have that any other subsequence $p_{\epsilon j}$ converges to p. □

On the other hand, and taking advantage of the region under study we perform the spatial approximation by piecewise quadrangular Lagrange Q_1 finite elements. That is, p and ϑ are approximated as follows:

$$p \approx p_h = \sum_{j=1}^{n} N_j p_j, \tag{24}$$

$$\vartheta \approx \vartheta_h = \sum_{j=1}^{n} N_j \vartheta_j, \tag{25}$$

where sub-index h stands for the finite element approximation. Now, we solve by a fixed-point iteration the discretized problem:

$$\int_\Omega h^3 \nabla p_h^{n+1} \nabla \phi_h + \frac{1}{k} \int_\Omega \vartheta_h^{n+1} h \Lambda \phi_h = \frac{1}{k} \int_\Omega (\vartheta_h^n h \Lambda) \circ \chi^k \phi_h,$$

$$\vartheta_h^{n+1} = H_\epsilon(p_h^{n+1}), \tag{26}$$

which must minimize at each iteration the following functional:

$$J(p_h^{n+1}) = \frac{1}{2} \int_\Omega h^3 |\nabla p_h^{n+1}|^2 + \frac{1}{k} \int_\Omega h \Lambda \Phi_\epsilon(p_h^{n+1}) - \frac{1}{k} \int_\Omega (\vartheta_h^n h \Lambda) \circ \chi^k p_h^{n+1}. \tag{27}$$

To perform the minimization stage we use the algorithm L-BFGS [23], with the line search approach by Moré and Thuente [22]. The L-BFGS algorithm is useful in this case as we are dealing with a large scale problem whose Hessian matrix cannot be computed at a reasonable cost [23].

4 Inverse problem resolution

We first consider the balance of forces involved in the problem, see Sect. 2.2. We define the residual R as follows:

$$R(\eta, \alpha) = \begin{bmatrix} f_\theta - \int_\Omega p(\eta, \alpha, \theta, x) \cos\theta \mathrm{d}\theta \mathrm{d}x \\ f_x - \int_\Omega p(\eta, \alpha, \theta, x) \sin\theta \mathrm{d}\theta \mathrm{d}x \end{bmatrix}. \tag{28}$$

The numerical approach is to minimize the L^2-norm of the residual R in least squares sense, i.e. $min \|R\|_2^2$. We note that to obtain the pressure p, two unknown parameters are needed: $\eta \in [0, 1]$ and $\alpha \in [0, 2\pi)$ which determine the shaft position in the system. We use an iterative method in the set of admissible positions (η, α) in order to minimize $\|R\|_2^2$, where p is the solution to the hydrodynamic problem Eqs. (6–9) whose coefficients depends on η and α.

For the optimization routine we propose a trust-region algorithmic strategy [23]. Following the idea behind a trust-region method, the information gathered about R is used to construct an approximation of R in a neighborhood of d_k (the trust region) which we denote by m_k. We find the step $s_k = d_{k+1} - d_k$ by solving the following subproblem:

$$\min_{s_k \in I\!R^2} m_k(d_k + s_k), \quad \text{where} \quad d_k + s_k \quad \text{lies inside the trust region.} \tag{29}$$

Let He and G be defined by:

$$He(d_k) \stackrel{\text{def}}{=} \nabla^2 R(d_k), \qquad G(d_k) \stackrel{\text{def}}{=} \nabla R(d_k)$$

Then, let l and u be the lower and upper bounds of d_k, we define a vector function $r(d_k) : I\!R^n \to I\!R^n$ as follows:

Definition 1 The vector $r(d_k) \in I\!R^n$ is defined:

(i) if $G(d_k)_i < 0$ and $u_i < \infty$, then $r_i \stackrel{\text{def}}{=} (d_k)_i - u_i$,
(ii) if $G(d_k)_i \geq 0$ and $l_i > -\infty$, then $r_i \stackrel{\text{def}}{=} (d_k)_i - l_i$,

For any $a \in I\!R^n$, $diag(a)$ denotes an n-by-n diagonal matrix with the vector a defining the diagonal entries in their natural order. So, we define:

$$D(d_k) \stackrel{\text{def}}{=} diag\left(|r(d_k)|^{-\frac{1}{2}}\right).$$

In this manner and because we are facing a determined nonlinear system of equations and a bounded admissible set of parameters, we propose the following scaled trust-region subproblem as in [11].

$$\min_{s_k \in I\!R^2} m_k(s) \stackrel{\text{def}}{=} s_k^T G_k + \frac{1}{2} s_k^T M_k s_k$$

where

$$J^r(d_k) \stackrel{\text{def}}{=} diag(sgn(G(d_k))), \tag{30}$$

$$C(d_k) \stackrel{\text{def}}{=} D(d_k) diag(G(d_k)) J^r(d_k) D(d_k), \tag{31}$$

$$M(d_k) \stackrel{\text{def}}{=} B(d_k) + C(d_k), \tag{32}$$

where $B(d_k)$ is the discretization of He.

As the notation indicates, m_k and R are in agreement to first order at the current iterate d_k. The matrix M_k and the diagonal matrix D_k are chosen this way such that there is no need to handle constraints explicitly. Since the quadratic model m_k is defined to include the constraint information, a natural extension to the classical ρ_k definition (see [23]) also takes place and it is given by:

$$\rho_k \stackrel{\text{def}}{=} \frac{R(d_k + s_k) - R(d_k) + \frac{1}{2} s_k^T C(d_k) s_k}{m_k(s_k)}, \tag{33}$$

see [11] for a wide explanation on this selection. With this approach, it is possible to obtain an approximate trust-region solution which can guarantee second-order convergence by simply solving an unconstrained trust-region subproblem. Each iteration involves the approximate solution of the system using the method of preconditioned conjugate gradients. When the squared 2-norm of R is small enough in correspondence with the tolerance chosen the algorithm finishes.

5 Numerical results and discussion

The mathematical formulation of the cavitation free boundary problem of this research was performed by the well known Elrod–Adams model, which includes a nonlinear term given by the Heaviside function.

We considered a regularization of this function by a cubic interpolating Hermite polynomial, which allowed us to find a suitable convex functional to minimize, whose minimum is the solution to the penalized direct problem. The classical approach mentioned in Sect. 3.2, by the Yosida regularization, uses a different iterative procedure. The minimization stage was performed via the algorithm L-BFGS with the line search approach by Moré and Thuente [22].

Table 1 Geometrical, physical and numerical constants

Parameter	Symbol	Value
Journal bearing clearance	C	36×10^{-6}
Journal bearing length	L	1
Shaft radius	R_a	1
Feeding pressure	p_f	0.5
External force	$\|f\|$	3
Viscosity coefficient	μ	0.01
Heaviside approximation coefficients	ϵ	0.2
Initial eccentricity	η_0	0.3
Initial alpha coordinate	α_0	0

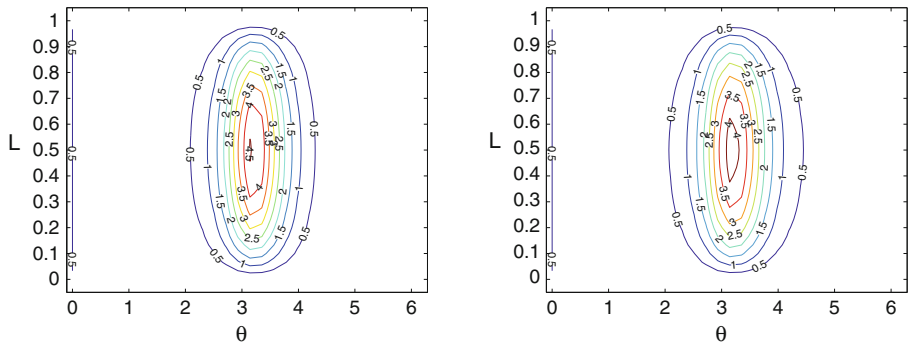

(a) Pressure contour map for $\epsilon = 0.2$

(b) Pressure contour map for $\epsilon = 0.05$

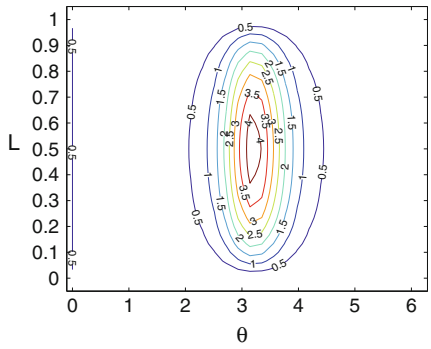

(c) Pressure contour map for $\epsilon = 0.001$

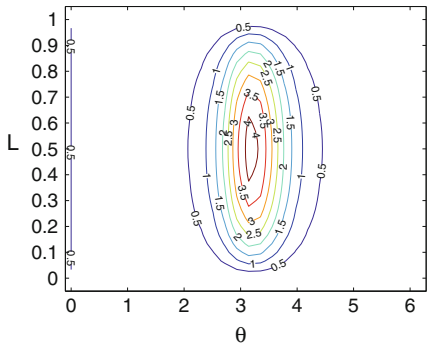

(d) Pressure contour map for $\epsilon = 0.0005$

Fig. 3 Dimensionless pressure contour maps for different ϵ values, for $\eta = 0.8$

In this section, we also present numerical tests which try to verify the performance and coupling of the different numerical approaches involved. For this, a 50×50 finite element regular mesh (2,500 rectangles with 4 nodes each) for $\Omega = [0, 2\pi] \times [0, \lambda]$ was used. Unless other values are specified, the geometrical, physical and numerical constants used during the experiments are those in Table 1. All constants are dimensionless.

In Fig. 3, different dimensionless pressure contour maps are presented. They show the behaviour of the solution of the direct problem (for $\eta = 0.8$) with respect to the penalization parameter ϵ, when it tends to zero. The ϵ values chosen for the experiment are

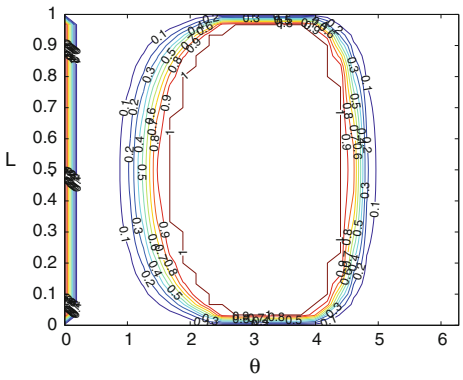

Fig. 4 The concentration contour map ϑ for $\epsilon = 0.2$ and $\eta = 0.8$

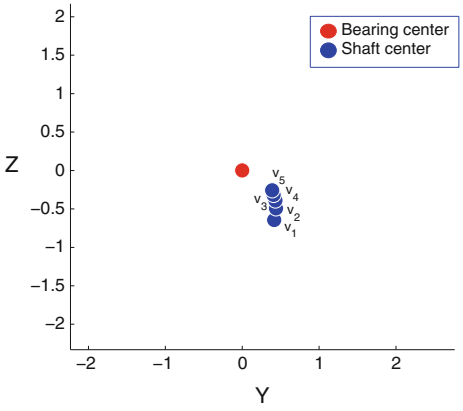

Fig. 5 The journal bearing equilibrium positions for $\vec{f} = (0, -3)$ and $v_1 = 1,\ v_2 = 2,\ v_3 = 3,\ v_4 = 4$ and $v_5 = 5$

0.2, 0.05, 0.001, 0.0005. Notice the stability of the contour map pattern when ϵ decreases. The results are similar to the ones obtained by Durany et al. [15] using a different strategy.

Figure 4 shows the concentration map related to Fig. 3a. Notice the concentration pattern on the groove supply.

For the resolution of the inverse problem, we introduced the residual function R in Eq. (28), which allowed us to find an easy way to pose the inverse problem as a constrained minimization problem. The choice of a trust-region algorithmic strategy to solve the problem allowed a solution where it is not necessary to handle constraints explicitly. Thus, it is possible to obtain an approximate trust-region solution which can guarantee second-order convergence by simply solving an unconstrained trust-region subproblem, see Sect. 3.2 for details.

Figure 5 shows the output of our whole numerical approach when a dimensionless force $\vec{f} = (0, -3)$ is applied to the journal bearing. The equilibrium positions are obtained for different velocities: $v_1 = 1,\ v_2 = 2,\ v_3 = 3,\ v_4 = 4$ and $v_5 = 5$.

Figure 6a shows the journal bearing equilibrium position when roughness is considered. For this case a force $\vec{f} = (0, -3)$ was also applied. The gap function used was: $h = 1 + \beta + \beta\cos(13\theta) + \eta\cos(\theta - \alpha)$ where β stands for the periodic roughness. The β value chosen was: 0.3. Figure 6b shows the response force disturbance depending on the journal bearing geometry with the same periodic roughness. Here, the direct problem is solved for shaft positions corresponding to $\alpha =$

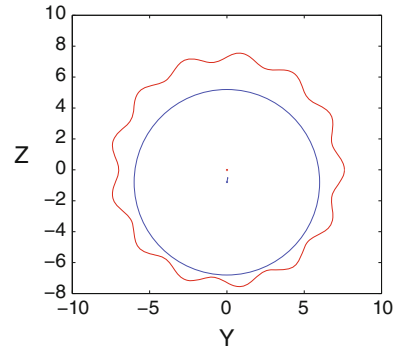

(a) Journal bearing reaction with roughness

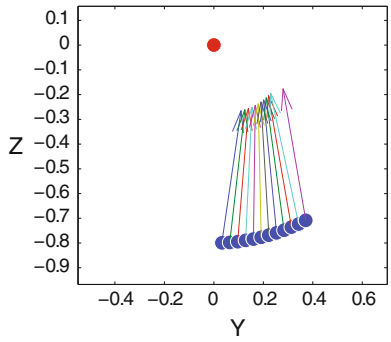

(b) Response force directions for a journal bearing with periodic roughness for $\alpha = 4.03e^{-02}$, $8.06e^{-02}$, $1.21e^{-01}$, $1.61e^{-01}$, $2.01e^{-01}$, $2.42e^{-01}$, $2.82e^{-01}$, $3.22e^{-01}$, $3.62e^{-01}$, $4.03e^{-01}$, $4.43e^{-01}$, $4.83e^{-01}$ and $\eta = 0.8$

Fig. 6 Simulation of a journal bearing with periodic roughness $\beta = 0.3$. For this case the gap function used was: $h = 1 + \beta + \beta\cos(13\theta) + \eta\cos(\theta - \alpha)$

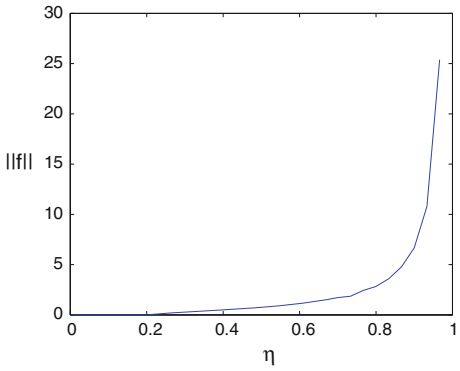

Fig. 7 The behaviour of η with respect to $\|f\|$

$4.03e^{-02}$, $8.06e^{-02}$, $1.21e^{-01}$, $1.61e^{-01}$, $2.01e^{-01}$, $2.42e^{-01}$, $2.82e^{-01}$, $3.22e^{-01}$, $3.62e^{-01}$, $4.03e^{-01}$, $4.43e^{-01}$, $4.83e^{-01}$ and $\eta = 0.8$.

Finally, Fig. 7 shows the behaviour of η with respect to $\|f\|$ at the equilibrium positions, illustrating how the eccentricity approaches to one when increasing the applied load. The simulation is taken for $h = 1 + \eta\cos(\theta - \alpha)$.

6 Conclusions

It is possible to find a numerical solution to the hydrodynamic Reynolds equation with the cavitation model of Elrod–Adams, under the assumptions made in this research, by minimizing the convex functional proposed in Sect. 3.3 for the direct problem.

It is possible to address the inverse problem related to this research by first posing a system of nonlinear equations and then solving it, in least squares sense, by a trust-region numerical approach. In this context, it provides another way of solution, different to the ones existing at this point.

The numerical simulations show that the force exerted by the pressure depends continuously on the geometry of the surfaces and the velocity of the shaft.

We note that, as $\|f\|$ increases, the eccentricity increases in a continuous and monotone way as far as the model is valid (i.e. for experimental values $|1-\eta| > 10^{-3}$).

Acknowledgments The first author was partially supported by the Institute for Interdisciplinary Mathematics (IMI), at the Complutense University of Madrid. The second author is partly supported by the project MTM2009-13655 Ministerio de Ciencia e Innovacion (Spain).

References

1. Bayada, G., Chambat, M.: Sur quelques modélizations de la zone de cavitation en lubrification hydrodynamique. J. Theor. Appl. Mech. **5**(5), 703–729 (1986)
2. Bayada, G., Chambat, M.: The transition between the Stokes equation and the Reynolds equation: a mathematical proof. Appl. Math. Optim. **14**(1), 73–93 (1986)
3. Bayada, G., Chambat, M., Vázquez, C.: Characteristics method for the formulation and computation of a free boundary cavitation problem. J. Comput. Appl. Math. **98**(2), 191–212 (1998)
4. Bayada, G., Martin, S., Vázquez, C.: Homogneisation du modle d'Elrod-Adams hydrodynamique. J. Asymptot. Anal. **44**, 75–110 (2005)
5. Bayada, G., Martin, S., Vázquez, C.: An average ow model of the Reynolds roughness including mass-flow preserving cavitation. ASME J. Tribol. **127**(4), 793–802 (2005)
6. Bayada, G., Vázquez, C.: A survey on mathematical aspects of lubrication problems. Boletín de la Sociedad Española de Matemática Aplicada **39**, 37–74 (2007)
7. Bermúdez, A., Durany, J.: Numerical solution of cavitation problems in lubrication. Comput. Methods Appl. Mech. Eng. **75**, 455–466 (1989)
8. Bermúdez, A., Moreno, C.: Duality methods for solving variational inequalities. Comp. Math. Appl. **7**, 43–58 (1981)
9. Brézis, H.: Análisis Funcional. Alianza Editorial (1984)
10. Calvo, N., Durany, J., Vázquez, C.: Comparación de algoritmos numéricos en problemas de lubricación hidrodinámica con cavitación en dimensión uno. Revista internacional de métodos numéricos para cálculo y diseño en ingeniería **13**(2), 185–209 (1997)
11. Coleman, T., Li, Y.: An interior trust region approach for nonlinear minimization subject to bounds. SIAM J. Optim. **6**, 418–445 (1996)
12. Dowson, D.: A generalized Reynolds equation for fluid film lubrication. Int. J. Mech. Sci. **4**, 159–170 (1962)
13. Dowson, D., Taylor, C.: Cavitation in bearings. Annu. Rev. Fluid Mech. **11**(1), 35–65 (1979)
14. Durany, J., Garcia, G., Vázquez, C.: Numerical simulation of a lubricated Hertzian contact problem under imposed load. Finite Elem. Anal. Des. **38**(7), 645–658 (2002)
15. Durany, J., Pereira, J., Varas, F.: Numerical solution to steady and transient problems in thermohydrodynamic lubrication using a combination of finite element, finite volume and boundary element methods. Finite Elem. Anal. Des. **44**(11), 686–695 (2008)
16. Durany, J., Pereira, J., Varas, F.: Dynamical stability of journal-bearing devices through numerical simulation of thermohydrodynamic models. Tribol. Int. **43**, 1703–1718 (2010)
17. Durany, J., Vázquez, C.: Numerical approach of lubrication problems in journal bearing devices with axial supply. Numer. Methods Eng. **92**, 839–844 (1992)
18. El Alaoui Talibi, M., Bayada, G.: Une méthode du type caractéristique pour la résolution d'un problème de lubrification hydrodynamique en régime transitoire. Modélisation mathématique et analyse numérique **25**(4), 395–423 (1991)
19. Elrod, H., Adams, M.: A computer program for cavitation. Cavitation and Related Phenomena in Lubrication, pp. 37–42. (1975)
20. Frêne, J., Nicolas, D., Degueurce, B., Berthe, D., Godet, M.: Hydrodynamic Lubrication: Bearings and Thrust Bearings, chap. 6. Elsevier Science, Amsterdam (1997)

21. Martin, S.: Influence of multiscale roughness patterns in cavitated flows: applications to journal bearings. Math. Probl. Eng. **2008**, 1–26 (2008)
22. Moré, J.J., Thuente, D.J.: Line search algorithms with guaranteed sufficient decrease. ACM Trans. Math. Softw. **20**, 286–307 (1994)
23. Nocedal, J., J. Wright, S.: Numerical Optimization. Springer Science + Business Media, LLC (2006)
24. Quarteroni, A., Sacco, R., Saleri, F.: Numerical Mathematics. Springer, Berlin (2000)